ORIGINAL ARTICLE   **OPEN ACCESS**

Human Serum Albumin Nanoparticles for Use in Cancer Drug Delivery: *In Vitro* Characterization

*Mohini.Kovvuri[1], **Jayesh Dwivedi[2]**, **Ravindra.Nagasuri[3]**, **Udichi Kataria[4]**, **Hareesh.Dara[5]**
1.Research Scholar, Pacific Academy of Higher Education& Research University(PAHER),Udaipur.
2.Principal, Pacific College of Pharmacy, PAHER University ,Udaipur, Rajasthan.
3.Principal,MAK College of Pharmacy, Hyderabad
4.Professor and Head of the Department of Pharmaceutics ,Geetanjali Institute of Pharmacy,Geetanjali University,Udaipur,Rajasthan.
5.Professor,Sree College of Pharmacy,Kothagudem.

ABSTRACT
Human serum albumin nanoparticles (HSA-NPs) are widely-used drug delivery systems with applications in various diseases, like cancer. For intravenous administration of HSA-NPs, the particle size, surface charge, drug loading and in vitro release kinetics are important parameters for consideration. This study focuses on the development of stable HSA-NPs containing the anti-cancer drug Ibrutinib (ITB) via the emulsion-solvent evaporation method using a high-pressure homogenizer. The key parameters for the preparation of ITB-HSA-NPs are: the starting concentrations of HSA, PTX and the organic solvent, including the homogenization pressure and its number cycles, were optimized. The mean particle size of the optimized formulation of Ibrutinib loaded nanoparticles was found to be 226.72±4.1 nm and span value of 0.22 whereas, that of optimized glutathione conjugated Ibrutinib loaded nanoparticles was found to be 226.72±4.8 nm and span value of 0.24.The results of in vitro release studies suggest that the release was more at pH 4.0 as compared to pH 6.0 and 7.4 exhibiting good release behavior in brain microenvironment pH.In summary, all parameters involved in HSA-NPs' preparation, its anticancer efficacy and scale-up are outlined in this research article.
Keywords: human serum albumin; nanoparticles; Ibrutinib; cancer; MCF-7

INTRODUCTION

Cancer is one of the leading causes of mortality and morbidity across the world. To date, the most common treatments for cancer include radiation therapy, chemotherapy and surgery [1]. However, their benefits are outnumbered by their disadvantages, such as renal toxicity, hepatic toxicity or lower availability of the drug at the target site [2]. These problems can be addressed by using a target-specific and biocompatible drug delivery vehicle, such as human serum albumin [3–5]. Human serum albumin (HSA) is the most abundant protein found in the human body with a molecular weight of 66.5 kDa. It is produced by the liver and has a half-life of around 19 days [6]. As revealed by X-ray structure analysis, the structure of HSA comprises of three domains: I, II and III. Each of these domains consists of two subdomains (Ia, Ib, IIa, IIb, IIIa and IIIb), which are arranged together to form binding sites on the HSA molecules [7]. HSA can bind to metabolic substrates, as well as therapeutic drugs, which include hydrophobic as well as hydrophilic drugs. HSA-NPs are formed by the aggregation of HSA molecules in solution forming intermolecular disulfide bonds [8].The properties of HSA-NPs include biocompatibility, biodegradability and non-immunogenicity [4,9]. The target specificity of HSA for the glycoprotein60 (gp60) receptor present on the surface of cancer cells, allows the delivery of various anti-cancer drugs, such as docetaxel [10], Ibrutinib [11] and noscapine [4], without inducing an immune response [5,9]. Ibrutinib is an anti-cancer drug widely used as a chemo-therapeutic agent for the treatment of different cancer types, such as breast, ovarian and lung cancer [12,13]. Due to the toxic effects of this formulation on normal cells, Ibrutinib was used in combination with HSA-NPs for site-specific delivery [12,14,15]. This has led to improved tumor targeting by enhancement of the enhanced permeability and retention (EPR) effect as opposed to administration of free drugs [15].

The retention of these colloidal drug delivery systems within the body is highly influenced by the particle's size, physical stability and surface characteristics [16]. It is known that nanoparticles in the size range 10–100 nm enter the lymphatic capillaries and undergo clearance [17]. Furthermore, particles in the size range of 250 nm–1 μm are identified by macrophages and removed by the reticuloendothelial system (RES) by the process of opsonization. This is a mechanism by which macrophages or monocytes identify and remove target cells or particles from the body by binding to them [17,18]. A lower surface curvature of the nanoparticles also lowers their chances of opsonization. This process is also influenced by the zeta potential of the particles. Negatively-charged particles prevent nanoparticle aggregation, whereas positively-charged particles promote binding to opsonin molecules, leading to their removal from blood circulation [19]. Thus, it is essential to control the particle size and zeta potentials of HSA-NPs to prevent their removal and ensure maximum efficacy.

MATERIAL ANDMETHODS
Materials
Human Serum Albumin IP (20% total protein) was procured from Reliance Life Sciences Pvt. Ltd. Navi Mumbai. Ibrutinib, Glutathione (reduced) and EDAC was purchased from S. D. Fine Chem (India). Poloxamer 188, SLS and Tween 80 were supplied as a gift sample from Sandoz Pvt. Ltd, Mumbai. Glutathione (reduced) and EDAC was purchased from S. D. Fine Chem (India). DCM (purity NLT 99% by GC), Acetone (purity NLT 99% by GC), methanol (HPLC grade) and ethanol were procured from Merck and co, Germany. Glutaraldehyde was purchased from SD fine chem, Mumbai. Double distilled water used was filtered through 0.22μm filter from Millipore (Mumbai, India) All other cited chemicals used were of analytical grade.

Preparation of Ibrutinib loaded HSA nanoparticles
Ibrutinib loaded HSA nanoparticles were prepared by employing desolvation technique (Marty et al. 17–23; Langer K et al. 169-80). Definite amount of HSA was prepared in 20 mL of double distilled water containing known concentration of surfactant. A specified amount of desolvating agent containing Ibrutinib was added drop wise to the above aqueous solution containing polymer HSA. The mixture was stirred using blade homogenizer at 2500±200 rpm for 15 minutes (Remi equipments, Mumbai, India). Later, crosslinking was achieved by addition of glutaraldehyde in drop wise manner and the resultant nanoparticles dispersion was kept under stirring at room temperature for 6 hours for evaporation of organic solvent from the system and to facilitate crosslinking of polymer. Finally, the nanoparticles were obtained by drying in vacuum dryer.

Conjugation of glutathione with HSA nanoparticles
The procedure for conjugation of glutathione with HSA nanoparticles was same as used for the conjugation of glutathione with PLGA nanoparticles .

Characterization of glutathione conjugated and unconjugated HSA nanoparticles
The glutathione conjugated and unconjugated HSA nanoparticles were characterized for the parameters as characterized for PLGA nanoparticles.

In vitro characterization of Nanoparticles
Process yield
The percentage of process yield of both conjugated and unconjugated PLGA nanoparticles was calculated by using the following formula:

$$\text{Percentage yield} = \frac{\text{Practicalyield}}{\text{Theoreticalyield}} \times 100$$

Entrapment efficiency
The amount of Ibrutinib entrapped inside the nanoparticles was estimated by determining the drug loading capacity of the PLGA nanoparticles. 20 mg of both conjugated and unconjugated nanoparticles were digested in extraction liquid (phosphate buffer pH 7.4)which dissolves only Ibrutinib excluding polymer fragment.
The extract containing polymer fragments were separated using centrifugation for 15-20 minutes at 3500 rpm. Later the fluorescein content was determined in the supernatant layer using spectrofluorimeter .(Jasco Ltd, Japan (Chin et al. 1-8).
The percentage of entrapment efficiency was determined by using the formula:

$$\text{Percentage entrapment efficiency} = \frac{\text{Total amount of drug loaded}}{\text{Amount of drug added}} \text{ X } 100$$

Particle size and size distribution analysis
The average particle size and size distribution of Ibrutinib loaded PLGA nanoparticles was determined using particle size analyzer which works on the principle of dynamic light scattering technique (Nanophox, Sympatec GmbH, System- Partikel- Technik, Clausthal- Zellerfeld, Germany). The measurements recorded indicate average volume mean diameter 30 of samples conducted in triplicate. 5g of the prototype nanoparticulate formulation was diluted in 100 mL of double distilled water and sonicated for about 3-5 minutes to declump the aggregates and the resulted dispersion was analyzed for particle size at 25^0C. The width of the particle size distribution is articulated by means of span value (equation 6.3) which can be calculated by using formula (14,20)

$$\text{Span value} = \frac{D90 - D10}{D50}$$

Zeta potential analysis
Zeta potential refers to the charge on the surface of the nanoparticles which in turn plays a pivotal role in the stability of colloidal dispersions. The zeta potential value designates the extent of repulsive forces between the particles in dispersion which aid in preventing the agglomeration of particles upon storage. Lower zeta potential value leads to flocculated dispersion as the attractive forces dominate the repulsive forces and the particles unite to form aggregates. Zeta potential of the Ibrutinib loaded PLGA nanoparticles was analyzed using Zetasizer Nano (Malvern instruments, UK) by dispersing the sample in double distilled water followed by gentle sonication for deaggregation of particles.

Quantification of glutathione in conjugated PLGA nanoparticles by Ellman's assay
Ellman's reagent (5,5'-dithiobis-(2-nitrobenzoic acid) or DTNB) is used to quantitatively determine the number of glutathione units conjugated on the surface of each nanoparticle surface. Ellman's reagent was added to 5mL of phosphate buffer pH 7.2 containing 60 mg of conjugated and un-conjugated nanoparticles and 1mM EDTA and kept for 15-20 minutes at room temperature. The supernatant was collected by centrifugation for 15-20 minutes at 3500 rpm and the thiol content was estimated spectrofluorometrically after addition of 2mL of sodium hydrogen phosphate (0.2 M) against unconjugated nanoparticles as blank.
The number of glutathione units conjugated on the surface of the PLGA nanoparticles was calculated by using the formula (equation) (21):

$$n = aN \left[d \left(\frac{4}{3} \right) \pi r^3 \right]$$

Where, n= thiol functionality of glutathione unit per nanoparticle; a= mole of thiol per gram of PLGA; d= Density of nanoparticles; r= mean radius of nanoparticles and N= 6.011×10^{23} (Avogadro number). Density of PLGA nanoparticles was determined by mercury porosimetry analysis and the size, shape and diameter of the nanoparticles was obtained from laser light scattering studies.

***In vitro* release study**
The *in vitro* release of Ibrutinib from optimized PLGA nanoparticles was performed using dialysis bag technique. Dialysis bag (Himedia, molecular weight cut-off 12000 Da, Mumbai, India) was activated by soaking in the release medium overnight. Phosphate buffer pH 6.0 + 0.5% SLS, pH 4.0 + 0.5% SLS and pH 7.4 + 0.5% SLS were used as diffusion media which mimics the nasal mucosal microenvironment pH, brain microenvironment pH as well as physiological pH, respectively. The brain targeted polymeric nanoparticles, administered via intra-nasal route, enter the systemic circulation from the nasal mucosa and later reach the brain. Hence, the release behavior of the nanoparticles is studied at the respective pH. Nanoparticles equivalent to 5 mg of Ibrutinib were placed in the dialysis bag and immersed in the release medium after sealing both the ends with clips and kept at 37^0C under continuous stirring at 75 rpm. 2 mL aliquots were withdrawn from the medium at predetermined intervals of time, filtered with 0.45 µ polytetrafluoroethylene membrane filters and assayed for drug content spectrofluorometrically (22). Same amount of diffusion medium was replenished in order to maintain the sink condition to promote diffusion of drug into surrounding medium. Further the release model kinetics was determined by using DD solver add in program.

***Ex vivo* permeation study**
The permeability potential of PLGA nanoparticles conjugated with glutathione was assessed by e*x vivo* studies on sheep nasal mucosa which was procured from animal slaughter house. In order to correlate the *in vitro* release behavior of Ibrutinib from PLGA nanoparticles, e*x vivo* studies were performed

using Franz diffusion cell. The receptor compartment was filled with phosphate buffer pH 6.0 + 0.5% SLS and the nasal mucosa was mounted on the receptor compartment on which the optimized formulation was placed and the study was performed at 37ºC, 50-100 RPM. Phosphate buffer pH 6.0 was selected for the study as it mimics the nasal environment pH. Periodically at predetermined intervals of time, 2 mL of sample was withdrawn from the receptor compartment and subsequently replenished with fresh buffer solution to maintain sink condition. Further, the samples were diluted appropriately and analyzed spectroflurometrically against blank nanoparticles. The amount of Ibrutinib released from the formulation at different time points was calculated and the order of release kinetics was calculated (23).

In vivo biodistribution study

The targeting efficiency of glutathione conjugated PLGA nanoparticles following nasal administration was investigated in rats. A total of 18 healthy adult wistar rats each weighing around 200-350 g was used for the study. The animal studies were conducted as per the protocol and guidelines approved and laid down by the Institutional animal ethics committee (IAEC) and Committee for the Purpose of Control and Supervision of Experiments on Animals (CPSCEA) guidance. Animals were kept in large spacious cages to provide enough movement of animal and were sufficiently fed with food and water and maintained on 12:12 hours light/dark cycle. The rats were divided into three groups representing six animals in each group. First group was kept as control and received plain Ibrutinib solution. Group II received Ibrutinib loaded PLGA nanoparticles whereas the Group III with glutathione conjugated Ibrutinib loaded PLGA nanoparticles. In the experimental context, the formulations were administered intranasally at a dose of 2 mg/kg body weight of Ibrutinib (19). During nasal administration, the animal was held in the back in slant posture and the formulation was administered in each nostril swiftly using micropipette attached with LDPE tubing, having 0.1 mm internal diameter at the delivery site, thus allowing the animal for proper breathing. (Abdelbary et al. 300-10) One hour past intranasal administration of formulation, the biodistribution study was evaluated by checking the uptake of Ibrutinib by different organs like brain, liver, spleen, lungs and kidneys. Hence, the animal was sacrificed and the organs are separated and washed completely with phosphate buffer saline pH 7.4 in order to isolate all the adsorbed fluorescein and is stored at -20ºC for further studies. The organs separated were then homogenized in phosphate buffer saline pH 7.4 for fluorescein extraction from the organs. Later the suspension was centrifuged and the supernatant obtained was quantified spectroflurometrically to analyze total amount of fluorescein distributed in the organs (24).

Statistical analysis

All the experiments were performed in triplicate and the results obtained are presented as mean ± SD of the population. One way Analysis of variance (ANOVA) and regression analysis was performed to evaluate the statistical significance of the differences byconsidering $p<0.05$ for demonstrating statistically significant procedure. All the statistical evaluations were conducted using Minitab®16 statistical software (USA).

Stability study

Stability study of the optimized nanoparticles was carried out for a period of six months. Nanoparticles were transferred to vials and subsequently sealed and kept in stability chamber with temperature of 25ºC±2 ºC and 60% ± 5% RH (16). The nanoparticles were sampled at regular intervals of time (0, 3 and 6 months) for any change in particle size, morphology, PDI, zeta potential and drug content. In addition to these parameters, the physical appearance and the reconstitution properties were also evaluated (17,18).

RESULTS ANDDISCUSSION

Physicochemical properties of Ibrutinib loaded HSA nanoparticles

HSA nanoparticles were prepared by employing desolvation technique where Ibrutinib was encapsulated in the nanoparticles. As discussed earlier in formulation of PLGA nanoparticles, (section 6.4.1), various formulation variables such as concentration of albumin, ratio of Ibrutinib to HSA, concentration of poloxamer 188, stirring speed, pH of the system and amount of glutaraldehyde were studied and its influence on the particle size and entrapment efficiency of nanoparticles was evaluated as tabulated in table 6.04. The percentage process yield of the optimized formulation was found to be 89 ±3.8 %. The mean particle size of the optimized formulation of Ibrutinib loaded nanoparticles was found to be 226.72±4.1 nm (figure 6.08) and span value of 0.22 whereas, that of optimized glutathione conjugated Ibrutinib loaded nanoparticles was found to be 226.72±4.8 nm and span value of 0.24 as shown in figure 6.09. A direct relationship between concentration of HSA and particle size was observed i.e. on increasing the polymer concentration from 10 mg/mL to 20 mg/mL, the particle size was found to increase proportionately from 215.02 ±6.8 nm to 229.12±5.5 nm. This can be attributed to the increase in viscosity due to high polymer concentration which resulted in a higher mass transfer resistance, thereby leading to larger particles (Schnurch AB,etal.95-103). Apart from polymer

concentration, rate of stirring was also found to affect the particle size of the formulation. Increasing the stirring rate from 1000 RPM to 2500 RPM led to the decrease in particle size from 256.9±6.6 nm to 226.72±4.8 nm due to increase in mass transfer at higher rates of stirring thereby, enhancing the diffusion between multiphase and rapid nucleation leading to smaller particles.

Table 1. Screening of process variables for optimization of Ibrutinib loaded HSA nanoparticles.

Process Variable	Variable value	% Entrapment efficiency	% process yield	Particle size (nm)	Zeta potential (mV)
Concentration of HSA	10 mg/mL	51.1±4.3	88.12±3.3	215.02±6.8	-40.4±2.2
	15 mg/mL	52.2±4.6	89.01±3.8	224.61±5.8	-41.2±2.6
	20 mg/mL	53.05±4.2	89.98±4.2	229.12±5.5	-41.7±2.4
Ibrutinib : HSA	1:05	49.79±4.6	84.22±4.6	207.6±5.2	-41.1±1.8
	1:10	54.11±3.8	87.39±3.8	228.8±5.5	-41.5±2.3
	1:15	54.8±3.4	88.18±3.4	249.21±5.6	-41.8±2.5
Stirring speed	1000 RPM	47.71±4.9	85.26±5.8	256.9±6.6	-39.5±2.8
	1250 RPM	51.19±4.1	86.12±4.6	242.29±5.8	-39.8±2.6
	2500 RPM	53.9±3.3	88.06±3.1	226.72±4.8	-39.6±1.8
Concentration of poloxamer 188	0.1 %w/w	52.32±4.2	86.45±3.6	228.2±4.0	-42.5±1.8
	0.2 %w/w	51.61±4.4	87.12±4.4	195.25±3.8	-41.4±2.6

Conjugation of glutathione with Ibrutinib loaded HSA nanoparticles
As discussed earlier in the Ibrutinib loaded HSA nanoparticles, the Glutathione was conjugated on the surface of the nanoparticles by using two step carbodiimide chemistry using EDAC as linker and quantified using Ellman's assay as shown in table 6.05. The amount of glutathione was optimized as 150 mg for conjugation reaction and the particle size was determined to assess the influence of glutathione conjugation on particle size of nanoparticles. From the results, it was found that the particle size of nanoparticles increased to 229.03 ± 4.8 nm after conjugation reaction with span value of 0.37. The optimized formulation exhibited 591.43±136 units of glutathione conjugated per nanoparticle (table6.05).

Table 2. Influence of EDAC concentration on conjugation of glutathione with HSA nanoparticle.

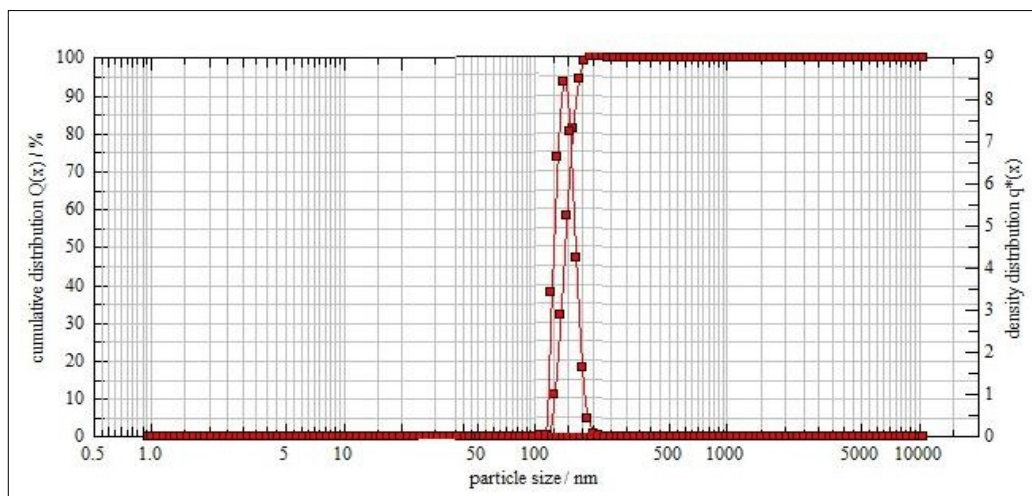| Amount of EDAC per 100mg of HSA nanoparticles	Thiol groups µmol/g of HSA	Thiol groups per HSAnanoparticle	Particle diameter (nm)	Zeta potential (mV)
150 mg	30.14±8.26	558.13±128	216.32± 4.4	-42.4±1.6
200 mg	29.12±8.78	591.43±136	228.72±4.8	-41.9±1.4

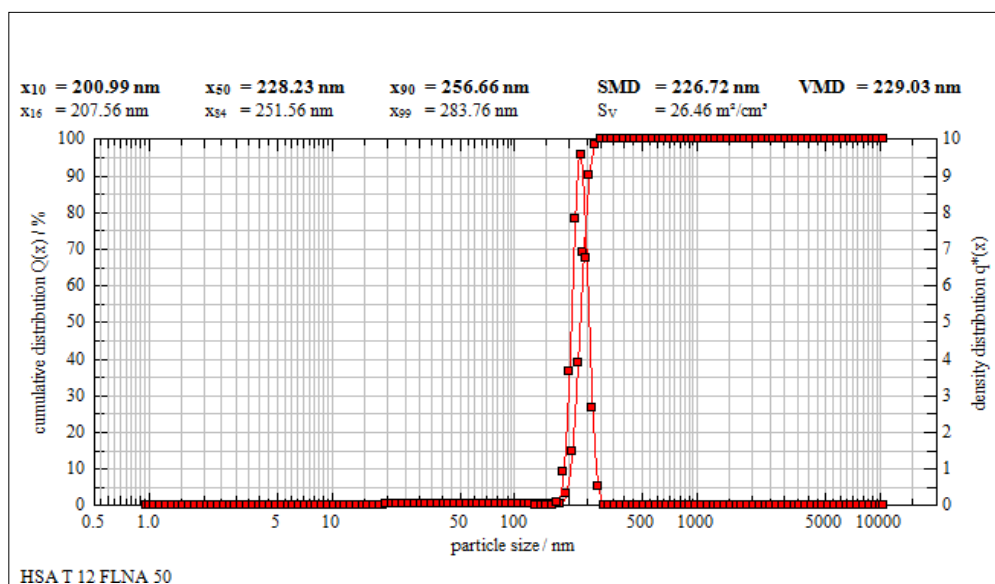Figure 1. Particle size report of Ibrutinib loaded HSA nanoparticles.

Figure 2. Particle size report of glutathione conjugated Ibrutinib loaded HSA nanoparticles.

In vitro release studies and *Ex vivo* release studies

The *in vitro* release studies were conducted using dialysis bag method using phosphate buffer pH 4.0, 6.0 as well as 7.4 + 0.5% SLS as diffusion medium as it simulates the pH of brain microenvironment pH, nasal microenvironment and physiological pH, respectively. The results indicated a biphasic release pattern (as shown in figure 3) with an initial burst release due to adsorbed Ibrutinib on the nanoparticle surface. Subsequently, this release behavior was followed by slow sustained release of Ibrutinib over a period of 24 hours which can be due to slow erosion of the polymer matrix releasing Ibrutinib in a controlled manner. The results of *in vitro* release studies suggest that the release was more at pH 4.0 as compared to pH 6.0 and 7.4 exhibiting good release behavior in brain microenvironment pH. The *in vitro* release of HSA nanoparticles followed best fit for Weibull model.

The *ex vivo* studies were conducted by mounting sheep's nasal mucosa on franz type diffusion cell with phosphate buffer pH 6.0 + 0.5 % SLS in the receptor compartment. Analogous to *in vitro* behavior, the results in *ex vivo* studies reveal biphasic release pattern with initial burst release followed by sustained release over a period of 24 hours as shown in figure 4. The permeability potential of glutathione conjugated nanoparticles was found to be more when compared to unconjugated nanoparticles, thus proving the permeability enhancing potential of glutathione. This can be attributed to the fact that glutathione aids in opening of tight junctions of the mucosal membrane as well as promoting the paracellular transport of molecules across mucosal membrane (Nagpal K, et al. 258-72). The glutathione conjugated and unconjugated HSA nanoparticles unveiled best fit for Weibull model.

In vivo biodistribution studies

The *in vivo* bio distribution studies of the formulation were evaluated in terms of uptake of the formulation by different organs (µg/g organ weight) one hour post intra-nasal administration in wistar rats. Around 1.60 µg of fluorescein per gram of brain was achieved by Ibrutinib loaded glutathione conjugated HSA nanoparticles which was significantly higher ($p<0.001$) than unconjugated HSA nanoparticles (1.18 µg/g) and plain Ibrutinib solution (0.72 µg/g of brain). Apart from the uptake of formulation by brain, the uptake and accumulation of formulation in the liver was also estimated (figure 5) and it was found that the Ibrutinib loaded glutathione conjugated nanoparticles exhibited reduced accumulation (2.72±0.057 %/g of liver) as compared to unconjugated HSA nanoparticles (2.78±0.003 %/g) and plain Ibrutinib solution (2.67±0.01 %/g).
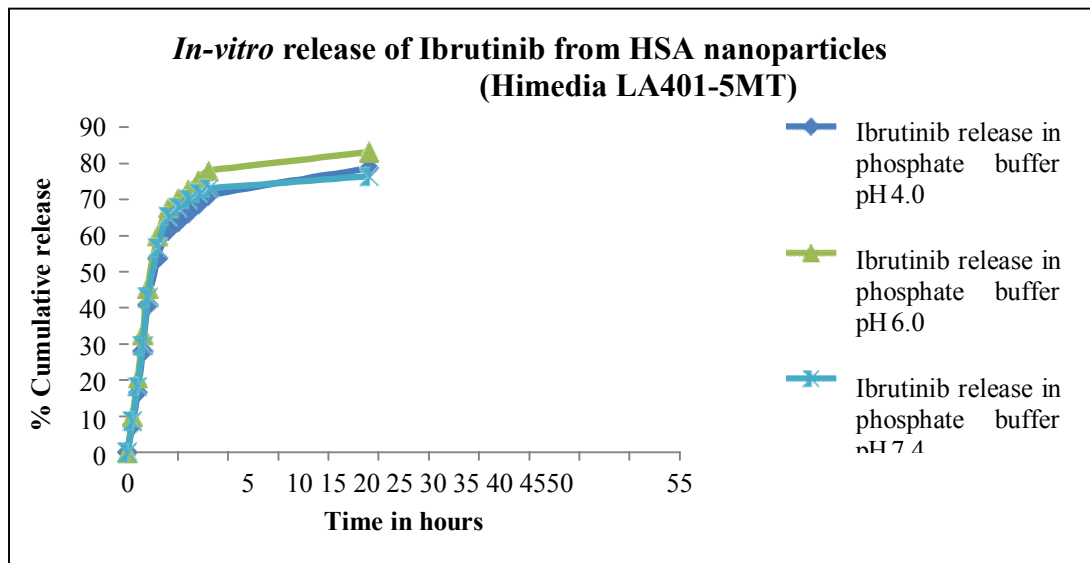
Figure 3.*In vitro* release profile of Ibrutinib from HSA nanoparticles at different dissolution media.
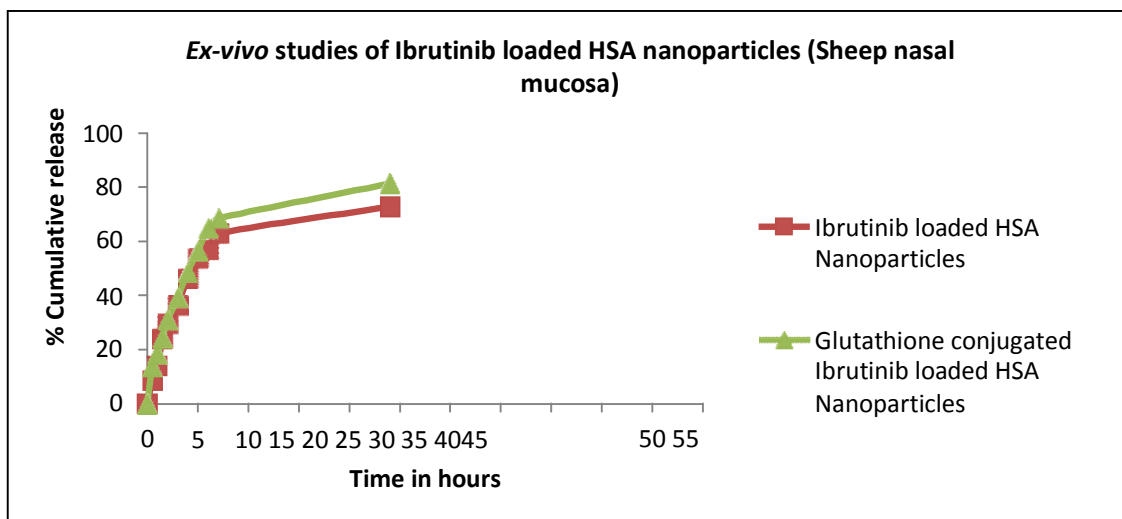

Figure 4 *Ex vivo* release of Ibrutinib from Glutathione conjugated and un-conjugated HSA nanoparticles.

The distribution of Ibrutinib to the brain was approximately 2.2 folds as compared to plain Ibrutinib and 1.35 folds as compared to unconjugated nanoparticles. The particle size of the formulation plays a crucial role in bio distribution of potential of the formulation and in interaction with cell membrane. The miniscule particle size (229.03 ±4.8nm) of the conjugated form of HSA nanoparticles is believed to be an important factor in achieving considerable amounts of Ibrutinib in brain. Further, the accumulation of fluoresce in the liver was found to be decreased with glutathione conjugated formulation. This reflects the permeability potential of the glutathione for effectively delivering the formulation across the BBB. Hence, as discussed earlier, glutathione is proven to be a ubiquitous thiol for its delivery potential across BBB into the brain and able to deliver the drug for therapeutic indication.

Stability studies

The stability studies were performed by storing the optimized formulation at 25ºC ± 2ºC/60% RH ± 5% RH for a period of six months in stability chamber. The formulation was evaluated for particle size, dispersibility and physical appearance of nanoparticles at 0, 3 and 6 months during storage. No significant difference was observed in the appearance of nanoparticles. The particle size seemed to increase which is assumed to be due to the aggregation of nanoparticles, which were subsequently dispersed after reconstitution. The similarity factor (*f2*) for the *in vitro* drug release studies found to be in specified range, thus signifying a stable formulation.

Table 3. Concentration of Ibrutinib (µg/g organ weight) in different organs following intra nasal administration of HSA nanoparticles for biodistribution study.

Organ	% Ibrutinib per gram of organ (Average ±SD)		
	F-Na	F-Na+HSA	F-Na+HSA+Glut
Blood	0.93±0.007	1.23±0.012[a]	1.18±0.016 [b]
Brain	0.36±0.02	0.59±0.021 [a]	0.80±0.017 [b]
Lung	1.70±0.09	1.54±0.004 [a]	1.77±0.030 [b]
Liver	2.67±0.01	2.78±0.003 [a]	2.72±0.057 [b]
Spleen	0.93±0.003	0.43±0.005 [a]	0.57±0.028 [b]
Kidney	2.96±0.001	1.97±0.004 [a]	1.58±0.027 [b]

Mean±SD (n=6).
[a]$p < 0.05$ Ibrutinib solution against Ibrutinib HSA NPs.
[b]$p < 0.001$ Ibrutinib HSA NPs against glutathione-conjugated Ibrutinib HSA NPs.

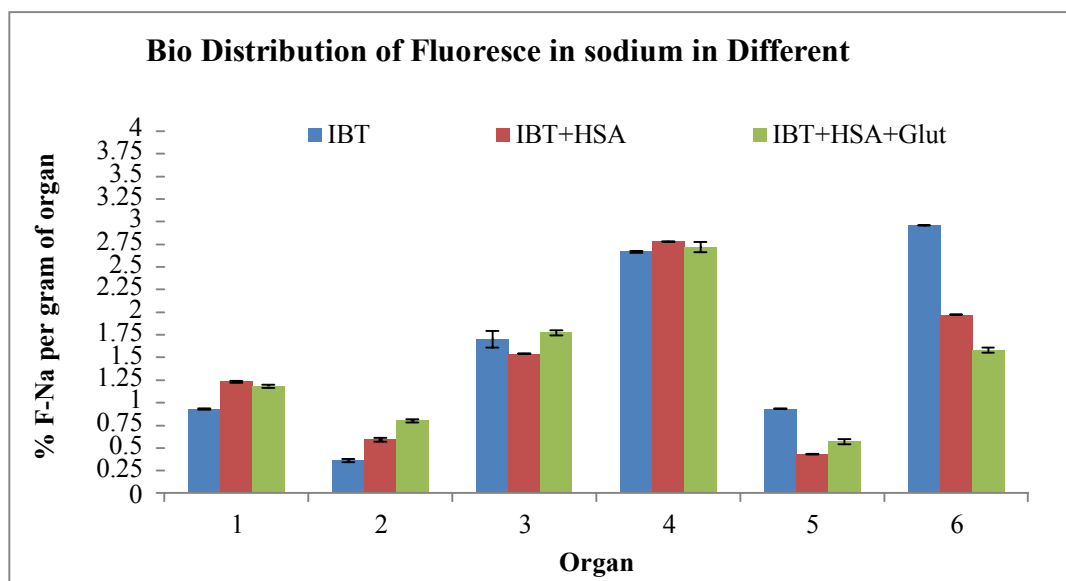

Figure 5 Ibrutinib (µg/g organ weight) in different organs following intra nasal administration of HSA nanoparticles for biodistribution study.

CONCLUSION

The current research was focused on the assessing the capability of glutathione as a ligand for enhancing the permeability of Ibrutinib to the brain. *In-vivo* studies results indicated that, transport of Ibrutinib to the brain via intranasal route is improved considerably in comparison to Ibrutinib solution and unconjugated polymeric nanoparticles. The transportation of the conjugated nanoparticles increased about 2.2-2.5 folds as compared to plain Ibrutinib and 1.35-1.4 folds as compared to unconjugated nanoparticles. The present investigation unveiled the competence of glutathione conjugated nanoparticulate formulation as a potential brain drug delivery platform which resulted in a better targeting as well as safe and efficacious treatment option for brain related disorders by illustrating with the successful delivery of a hydrophilic organic molecule, Ibrutinib, a cross BBB.

REFERENCES

1. Urruticoechea, A.; Alemany, R.; Balart, J.; Villanueva, A.; Viñals, F.; Capellá, G. (2010). Recent advances in cancer therapy: An overview. Curr. Pharm. Des., 16, 3–10. [CrossRef] [PubMed]
2. Lordick, F.; Hacker, U. (2015). Chemotherapy and Targeted Therapy, in Imaging of Complications and Toxicity following Tumor Therapy; Kauczor, H.-U., Bäuerle, T., Eds.; Springer International Publishing: Cham (ZG, Switzerland), pp. 3–15.
3. Jeong, K.; Kang, C.S.; Kim, Y.; Lee, Y.-D.; Kwon, I.C.; Kim, S. (2016). Development of highly efficient nanocarrier-mediated delivery approaches for cancer therapy. Cancer Lett. 374, 31–43. [CrossRef][PubMed]
4. Sebak, S.; Mirzaei, M.; Malhotra, M.; Kulamarva, A.; Prakash, S. (2010). Human serum albumin nanoparticles as an efficient noscapine drug delivery system for potential use in breast cancer: Preparation and in vitro analysis. Int. J. Nanomed. 5, 525–532.
5. Abbasi, S.; Paul, A.; Shao, W.; Prakash, S. (2012). Cationic albumin nanoparticles for enhanced drug delivery to treat breast cancer: Preparation and in vitro assessment. J. Drug Deliv. 2011, [CrossRef]

6. Kratz, F. Albumin as a drug carrier: (2008). Design of prodrugs, drug conjugates and nanoparticles. J. Control. Release 2008, 132, 171–183. [CrossRef] [PubMed]
7. Dockal, M.; Carter, D.C.; Rüker, F. (1999). The three recombinant domains of human serum albumin structural characterization and ligand binding properties. J. Biol. Chem. 274, 29303–29310. [CrossRef] [PubMed]
8. Elzoghby, A.O.; Samy, W.M.; Elgindy, N.A. (2012). Albumin-based nanoparticles as potential controlled release drug delivery systems. J. Control. Release, 157, 168–182. [CrossRef] [PubMed]
9. Haley, B.; Frenkel, E. (2008). Nanoparticles for drug delivery in cancer treatment. Urol. Oncol. Semin. Orig. Investig. 26, 57–64.
10. Nateghian, N.; Goodarzi, N.; Amini, M.; Atyabi, F.; Khorramizadeh, M.R.; Dinarvand, R. Biotin/Folate-decorated Human Serum Albumin Nanoparticles of Docetaxel: Comparison of Chemically Conjugated Nanostructures and Physically Loaded Nanoparticles for Targeting of Breast Cancer. Chem. Biol. Drug Des. 2016, 87, 69–82. [CrossRef] [PubMed]
11. Zhao, S.; Wang, W.; Huang, Y.; Fu, Y.; Cheng, Y. Paclitaxel loaded human serum albumin nanoparticles stabilized with intermolecular disulfide bonds. MedChemComm 2014, 5, 1658–1663. [CrossRef]
12. Dranitsaris, G.; Yu, B.; Wang, L.; Sun, W.; Zhou, Y.; King, J.; Kaura, S.; Zhang, A.; Yuan, P. Abraxane® versus Taxol® for patients with advanced breast cancer: A prospective time and motion analysis from a Chinese health care perspective. J. Oncol. Pharm. Pract. 2014, 22, 205–211. [CrossRef] [PubMed]
13. Abbasi, S.; Arghya, P.; Afshan, K.; Prakash, S. siRNA Delivery Using Biodegradable Nanoparticles for Breast Cancer Therapy. Nanotechnology 2016, 13, 74–76.
14. Desai, N.P.; Tao, C.; Yang, A.; Louie, L.; Zheng, T.; Yao, Z.; Soon-Shiong, P.; Magdassi, S. Protein Stabilized Pharmacologically Active Agents, Methods for the Preparation Thereof and Methods for the use Thereof. U.S. Patent 6749868 B1, 15 January 2004.
15. Maeda, H.; Wu, J.; Sawa, T.; Matsumura, Y.; Hori, K. (2000). Tumor vascular permeability and the EPR effect in macromolecular therapeutics: A review. J. Control. Release, 65, 271–284. [CrossRef]
16. Langer, K.; Baltasar, S.; Voqel, V.; Dinauer, N.; von Briesen, H.; Schubert, D.(2003). Optimization of the preparation process for human serum albumin (HSA) nanoparticles. Int. J. Pharm. 257, 169–180. [CrossRef]
17. Longmire, M.; Choyke, P.L.; Kobayashi, H. (2008). Clearance properties of nano-sized particles and molecules as imaging agents: Considerations and caveats. Nanomedicine (Lond.), 3, 703–717. [CrossRef] [PubMed]
18. Harashima, H.; Sakata, K.; Funato, K.; Kiwada, H. (1994). Enhanced hepatic uptake of liposomes through complement activation depending on the size of liposomes. Pharm. Res. 11, 402–406. [CrossRef][PubMed]
19. Owens, D.E.; Peppas, N.A. (2006). Opsonization, biodistribution, and pharmacokinetics of polymeric nanoparticles. Int. J. Pharm. 307, 93–102. [CrossRef] [PubMed]
20. Ranjan, A.P.; Mukerjee, A.; Helson, L.; Vishwanatha, J.K. (2012). Scale up, optimization and stability analysis of Curcumin C3 complex-loaded nanoparticles for cancer therapy. J. Nanobiotechnol. [CrossRef] [PubMed]
21. Ma, P.; Mumper, R.J. (2013). Paclitaxel nano-delivery systems: A comprehensive review. J. Nanomed. Nanotechnol. 4. [CrossRef] [PubMed]
22. Kim, T.H.; Jiang, H.H.; Youn, Y.S.; Park, C.W.; Tak, K.K.; Lee, S.; Kim, H.; Jon, S.; Chen, X.; Lee, K.C. (2011). Preparation and characterization of water-soluble albumin-bound curcumin nanoparticles with improved antitumor activity. Int. J. Pharm. 403, 285–291. [CrossRef] [PubMed]
23. Floury, J.; Desrumaux, A.; Lardieres, J. (2000). Effect of high-pressure homogenization on droplet size distributions and rheological properties of model oil-in-water emulsions. Innov. Food Sci. Emerg. Technol. 1, 127–134.[CrossRef]
24. Schultz, S.; Wagner, G.; Urban, K.; Ulrich, J. (2004). High-pressure homogenization as a process for emulsion formation. Chem. Eng. Technol. 27, 361–368. [CrossRef]

CITATION OF THIS ARTICLE
Mohini.Kovvuri,Jayesh Dwivedi, Ravindra.Nagasuri, Udichi Kataria, Hareesh.Dara. Human Serum Albumin Nanoparticles for Use in Cancer Drug Delivery: In Vitro Characterization. Bull. Env. Pharmacol. Life Sci., Vol 9[12] November 2020 : 60-68